

Kinetics of Competitive Adsorption of PEO Chains with Different Molecular Weights

Zengli Fu and Maria M. Santore*

Chemical Engineering Department, 111 Research Drive, Lehigh University, Bethlehem, Pennsylvania 18105-4791

Received January 13, 1998; Revised Manuscript Received July 30, 1998

ABSTRACT: Molecular weight driven competitive adsorption of PEO [poly(ethylene oxide)] from aqueous solutions on silica was studied by employing total internal reflectance fluorescence (TIRF) and near-Brewster angle reflectivity. Coumarin tags on PEO chain ends facilitated the distinction between two competing populations differing only in molecular weight. In gentle shearing flow, coadsorption was found to include three steps: independent transport-limited adsorption of both species, exchange of short and long chains, and the ultimate equilibration of the long chains. When the short chains are on the order of 30K and contact the surface for 20 min or less, their displacement by longer chains is transport-limited and approaches completion. However, for short chains of higher MW (120K), their displacement by longer chains becomes slow and less complete, indicating an energy barrier for short chain displacement. A kinetic model for competitive adsorption kinetics was proposed on the basis of the Langmuir adsorption kinetics and allowed quantification of surface limited kinetics.

Introduction

Competitive adsorption and exchange of macromolecules from solutions onto solid surfaces occurs in most applications where polymer adsorption is exploited. Even the simplest applications employing single homopolymer additives are influenced by issues of competitive adsorption, since polydisperse samples give rise to competition between short and long chains. Control of adsorbed layer properties requires knowledge of polydispersity-related kinetics, through which the interfacial molecular weight and the adsorbed layer properties evolve.

Early experimental studies qualitatively documented competitive adsorption and chain exchange processes;^{1,2} however, quantitative theoretical examination of multi-component polymer equilibria^{3,4} and surface sensitive measurements of the exchange kinetics^{5–12} have emerged only recently. Granick and co-workers observed that the replacement of adsorbed polystyrene (PS) by poly(methyl methacrylate) (PMMA) in organic solvents on oxidized silicon could take several hours.^{7,9} PS and PMMA are relatively rigid and have limited surface mobility. Therefore in these kinetic studies, the rate-controlling step must be at the surface, as opposed to bulk diffusion. In contrast, Dijt et al. showed that the displacement of short poly(ethylene oxide) (PEO) chains (7K MW) on silica by longer ones (400K MW) was completed within minutes, and the exchange rate was bulk diffusion controlled.¹¹ The fast surface kinetics were attributed to PEO's greater flexibility and surface mobility. Since only a limited number of systems have been studied, and since experimental restrictions limit the accessible range of kinetic data, the exact role of backbone stiffness, segment–surface contacts, and interfacial entanglements on competitive processes in adsorbed layers has yet to be understood.

PEO represents an interesting model system with which to probe dynamic issues, since it is thought to undergo rapid dynamics as a result of its low glass transition temperature and lack of side groups. Several groups document interfacial kinetics dominated by local

equilibrium;^{11,14} however, certain experimental histories may still cause deviations from local equilibrium. Because of PEO's relatively fast interfacial dynamics, one might expect that in such situations, the return toward equilibrium would be on an experimentally accessible time scale, providing insight into issues of interfacial relaxations. One scenario which we found to sometimes give deviations from local equilibrium was that of competitive adsorption between PEO chains of different lengths. Notably, equilibrium theories such as that of Scheutjens and Fleer³ predict that, for homopolymer chains differing only in length, complete preferential adsorption of the longer chains occurs (ultimately, at equilibrium) when the two molecular weights differ by a factor of 2 or more. This prediction has been confirmed experimentally for many systems, though for polymers that are slow to equilibrate on a surface, establishing the equilibrium surface composition is more difficult.

An understanding of competitive adsorption processes begins with a knowledge of the adsorption behavior of individual components. In the case of PEO adsorbing onto silica, kinetics are known to be transport limited up to as least 90% of coverage for shearing slit flow and impinging jet geometries.^{13,14} Furthermore, after the transport-limited surface saturation, there is no evolution in surface coverage, for periods up to 24 h.^{14,15} In fact, with narrow molecular weight PEO standards, the plateau of the isotherm has been shown to be relatively flat, with a coverage independent of the rate of chain arrival to the interface. Our prior studies did not probe interfacial chain configurations and therefore did not directly determine the extent to which adsorbed layers were truly "equilibrated"; however, the same adsorbed mass was always observed for a particular bulk solution concentration, independent of adsorption history of contact time. It would therefore appear that the use of "equilibrium adsorbed amount" is an adequate description of the surface mass.

Recent self-exchange studies have been conducted, in which preadsorbed PEO layers were later challenged

with labeled chains that were otherwise identical to those originally adsorbed.¹⁵ It was revealed that adsorbed PEO layers are initially in a highly mobile state where the interfacial mass and composition (labeled vs unlabeled) was described by transport-limited kinetics. After 10–20 h of aging, dynamics were sluggish and adsorbed chains were resistant to exchange with chains in the bulk solution. For the duration of the self-exchange studies, the overall mass stayed at the apparent equilibrium level, with no increase or overshoots. Therefore the PEO–silica–water system bears the striking feature that the evolution of the adsorbed mass frequently approached that predicted by equilibrium models, despite the continued evolution of the chain configurations and local dynamics. Clearly, the use of the term “equilibrium” depends on the sensitivity of the experimental techniques employed, since some features of adsorbed layer may be adequately described by their equilibrium values while others may not.

In competitive coadsorption runs with mixtures of short and long PEO chains, exchange was observed after surface saturation, driven by molecular weight differences.^{11,16} In the studies reported to date, which involved short chains of relatively low molecular weight, the exchange process appeared transport-limited, with local (mass and composition) equilibrium maintained at the interface. The extent to which this behavior occurs for different combinations of molecular weights has yet to be determined.

This work documents our findings for competitive adsorption between populations of PEO chains differing in molecular weight. Coadsorption kinetics are compared to sequential adsorption kinetics, where short chains are preadsorbed and later challenged by long chains. Several steps for simultaneous coadsorption are described, and the extent to which various steps maintain local equilibrium (fast interfacial kinetics) or are controlled by metastable states at the interface is discussed. A simple Langmuir model, including bulk solution transport and first-order surface kinetics, was proposed as a means of quantifying the various kinetics. The tendency for deviation from local equilibrium was found to be a strong function of the molecular weights of the competing species.

In this work, we employ end-labeled PEO chains to distinguish different molecular weight components during the competitive adsorption and exchange in mixtures containing several populations, each of narrow molecular weight distribution. While the total surface mass is measured by Brewster angle reflectivity, the adsorption of fluorescently labeled chains is monitored using total internal reflectance fluorescence (TIRF). The combination of two surface probes has advantages over studies that employ only a single method. For example, Dijt and co-workers¹¹ could, from their reflectometry data, deduce the molecular weight driven exchange process for molecular weight pairs in which the shorter chains were sufficiently short to give a significant difference in surface mass from that of the long chains. At high molecular weights, the influence of chain length on the equilibrium adsorbed amount is dramatically reduced, diminishing the utility of reflectivity in studies of competitive adsorption. For PEO adsorbing on silica, the influence of molecular weight on equilibrium coverage is reduced above molecular weights of 100K, such that in competitive situations, one cannot distinguish the contribution of the long and short chains by merely

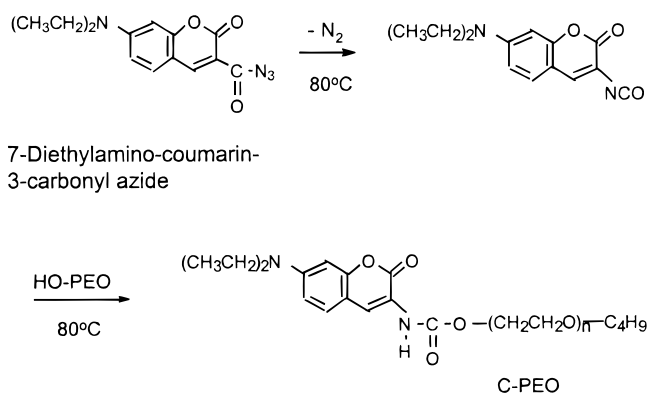


Figure 1. Labeling PEO chain end with coumarin dye.

examining the evolving surface mass or reflectivity signal. Therefore, population sensitive methods such as TIRF are of great utility in competitive adsorption studies.

Experimental Section

Adsorption Substrate and Flow Cell. Silica glass microscope slides (FISHER *finest*) were used as the adsorption substrate. Before the adsorption experiments, the glass substrate was treated by concentrated sulfuric acid for 15 h followed by flushing DI (deionized) water and pH 7 phosphate buffer to neutralize the surface. Analysis via XPS revealed that after this treatment, the glass surface composition was primarily SiO₂.¹⁷ Adsorption experiments were carried out by pumping polymer solutions through a thin rectangular flow channel with dimensions of 0.13 cm by 1.0 cm by 4.0 cm, using the glass surface as a wall of the flow cell. Kinetics at the center of the surface were monitored by the optical or fluorescence methods, described below. A wall shear rate of 7.2 s^{−1} on the adsorbing surface was used in the adsorption and exchange runs. Details of the flow cell assembling, cleaning, and experiment operation procedures have been described previously.^{14,17}

Coumarin Dye-Labeled PEO (C-PEO). We employed a coumarin label attached to one end on each PEO chain to identify interfacial populations of interest. In tagging experiments such as ours, care must be taken to minimize the potentially invasive effects of the label. To this end, coumarin was chosen because of its relatively low molecular weight (less than 300) and inclusion of some polar groups, which tend to reduce its hydrophobicity compared with more common labels such as pyrene or anthracene. In the Results, we also demonstrate that under the conditions of interest, the molecule is neutral, thereby avoiding electrostatic interactions near the silica surface.

Molecular weight standard PEO was purchased from Polymer Laboratories with sample molecular weights ranging from 33K to 960K and polydispersities of 1.1 or less. According to the supplier, the PEO chains contained an hydroxyl group at one end and a butyl group at the other. 7-(Diethylamino)-coumarin-3-carbonyl azide (the coumarin dye) was purchased from Molecular Probes, Inc. (Cat. no. D-1446) and was used to label PEO (MW 33K and MW 120K). Figure 1 shows the labeling reaction between the carbonyl azide group of the coumarin dye and the hydroxyl chain end of PEO. The reactions were conducted in toluene with about 15% of PEO. The hydroxyl/dye molar ratio was typically 1:2.5. The mixtures were allowed to react at 85 °C for 15 h while the solutions were gently stirred in an argon atmosphere. After the reaction, the polymer was precipitated in pentane.

Free dye was removed from the labeled sample by dissolving the reaction products in acetone and reprecipitating with pentane. Most of the free dye could be removed after several precipitation cycles. Samples to be characterized for labeling density were further purified by dialysis (in Spectra/Por

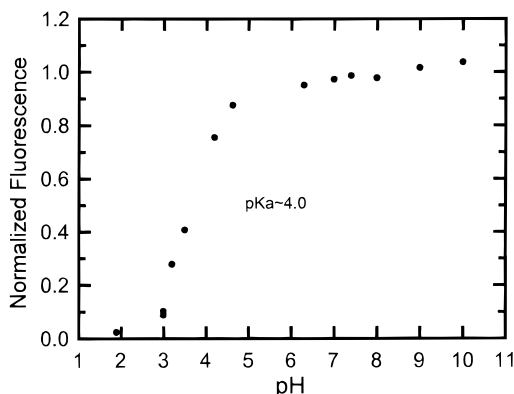


Figure 2. Fluorescence titration of C-PEO (33K MW). Bulk polymer solutions of 1 ppm concentration were excited by 405 nm light, and the emission intensity at 500 nm was measured.

membrane tube, molecular weight cutoff 6000–8000) against pH 7.1 phosphate buffer solution for 1 week.

The molecular weight distribution (MWD) of each C-PEO sample was compared with that of the corresponding native sample using gel permeation chromatography, and no significant change in MWD was detected. The fluorescent emission spectra (measured with 405 nm excitation light) of dilute C-PEO solutions in pH 7.1 phosphate buffer were identical in peak shape and position to that of free coumarin dye in the same buffer. The fraction of labeled chains in C-PEO samples was determined via absorbance, at 405 nm, of purified C-PEO solutions in buffer, with concentrations in the range 10–50 ppm. The calculation of labeling density was based on the comparison of the absorbance of the C-PEO solution of known polymer concentration with that of the standard solutions of free dye–ethyl diglycol ether ($\text{C}_2\text{H}_5\text{--O--C}_2\text{H}_4\text{--O--C}_2\text{H}_4\text{--OH}$) adduct. The C-PEO 33K MW and 120K MW samples used in this study had labeling densities of 95% and 93%, respectively.

The fluorescence intensities of bulk C-PEO 33K solutions (1 ppm) were measured as a function of pH with a SPEX Fluorolog spectrometer, and the result is shown in Figure 2. The fluorescence is quenched at acidic pH values due to the protonation of the diethylamino group in the coumarin dye. Figure 2 suggests a pK_a value of about 4, which is comparable to the pK_a value of (dimethylamino)naphthalene ($pK_a = 4.566^{18}$). Thus, around pH 7, where we conducted the adsorption studies, the coumarin dye is mostly unprotonated so that the tagged PEO chain ends are uncharged. The neutrality of the chain ends is significant in that neutral labels are less likely to alter the adsorption behavior through electrostatic interactions.

Adsorption Kinetics Measurements. Total internal reflectance fluorescence (TIRF) and near-Brewster angle reflectometry were run in parallel, using the adsorption flow cell described above. The adsorption of fluorescently labeled chains in a mixture of different components was tracked by TIRF, while the total surface mass was measured by reflectivity. Instrumental and calibration details for TIRF^{17,19,20} and reflectivity¹⁴ have been described previously. In TIRF experiments, the sample was illuminated with 405 nm light, which is close to the maximum absorption band for the coumarin dye, and the emission at 500 nm, close to the emission maximum, was detected. The penetration depth of the evanescent wave at the glass/water interface was between 80 and 130 nm, which was sufficiently large to provide complete illumination of the adsorbed polymer layer, giving a fluorescence signal proportional to the number of C-PEO chains. By controlling the penetration depth of the evanescent wave within the above range, the bulk solution contribution to the total TIRF signal was small (less than 5% of the maximum adsorption signal for 33K MW C-PEO at a concentration of 5 ppm and even smaller for 120K C-PEO at the same concentration). This fixed bulk contribution was subtracted at the beginning of TIRF adsorption traces. All the adsorption experiments used a dilute phosphate buffer (1 mM phosphate composed of

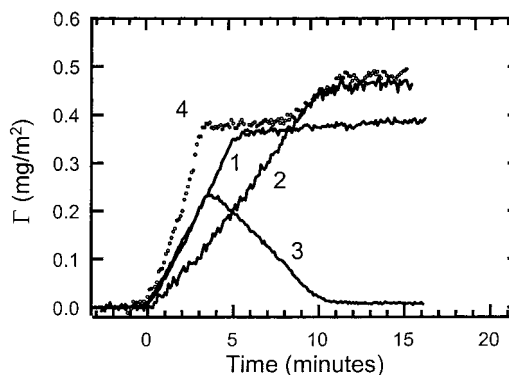


Figure 3. Competitive coadsorption and exchange kinetics for the 33K/120K MW PEO pair. Curve 1: noncompetitive adsorption from a 2.5 ppm solution of 33K PEO. Curve 2: noncompetitive adsorption from a 2.5 ppm solution of 120K PEO. Curve 3: coadsorption of C-PEO from a 50–50 wt % mixture of 33K and 120K PEO with a total concentration of 5 ppm. Curve 4: total surface coverage during coadsorption experiment of curve 3.

KH_2PO_4 and Na_2HPO_4 in 1:4 molar ratio) as the solvent to have a stabilized pH at 7.1.

The total adsorbed amount was measured by Brewster angle reflectivity. Single component adsorption measurements for C-PEO and native PEO revealed no measurable difference in the adsorption rates or the adsorbed amounts at saturation. This suggests that the effect of the labeled chain ends on the pure component adsorption was insignificant. In studies of mixtures, the amount of adsorbed C-PEO was determined by comparing the TIRF signal (after subtraction of bulk fluorescence) with that of a saturated C-PEO layer (of the same molecular weight), for which the adsorbed amount was known from reflectivity.

Results and Discussion

1. Competitive Adsorption of 33K PEO and Longer Chains. The competition between short and long chains was examined in two ways: First, mixtures of labeled short chains and unlabeled long chains were allowed to coadsorb. The labeled component on the surface was monitored by TIRF, and the evolving total surface mass was measured by reflectivity. Thus, the kinetics of the individual species in coadsorption were obtained. In the second type of study, the surface was initially saturated by the labeled short chains, and then the unlabeled longer chains were introduced into the flow cell. The displacement of the preadsorbed short chains was monitored by TIRF, while the total surface mass during the exchange was monitored by reflectivity.

(a) Coadsorption from Binary Mixtures. In Figure 3 the single component noncompetitive adsorption kinetics of 33K and 120K PEO are compared with their competitive coadsorption from a binary mixture of the two. Single component adsorption studies (curves 1 and 2) were conducted for free solution concentrations of 2.5 ppm. For the flow conditions in our cell and with dilute PEO solutions ($C_b < 20$ ppm), it has been verified¹⁴ that single species adsorption kinetics of monodisperse PEO samples obey the mass-transport-controlled rate law described by eq 1:

$$\frac{d\Gamma}{dt} = 0.538 \left(\frac{\gamma}{L} \right)^{1/3} D^{2/3} C_b \quad (1)$$

where γ is the wall shear rate, L is the distance from the entrance of the flow cell to the observation point on the surface, D is the diffusion coefficient of the adsorbing

species, and C_b is the bulk concentration. This mass-transport-limited rate persists up to 95% of full coverage.

In Figure 3, curve 3 tracks the evolving surface coverage of the 33K C-PEO chains adsorbing from a mixture of 33K C-PEO and unlabeled 120K PEO, where each component has a bulk solution concentration of 2.5 ppm. At short times, the short chain coadsorption rate (curve 3) is constant and equal to the mass-transport-limited rate observed for noncompetitive adsorption of the same short chains (in curve 1). In the late stages of coadsorption, the 33K C-PEO desorbs, leaving no short chains on the surface.

Curve 4 of Figure 3 illustrates the evolving total surface mass during the coadsorption run and includes an intermediate kinetic plateau in addition to the plateau representing the ultimate equilibrium coverage. Similar kinetic features were found by Dijt et al.¹¹ in their study of PEO mixtures (7K and 400K short and long chains, respectively) adsorbing onto an oxidized silicon wafer from aqueous solution. Our study explicitly demonstrates that the surface coverage of the intermediate plateau corresponds to the equilibrium coverage for noncompetitive short chain adsorption. Figure 3 also shows that the onset of the intermediate kinetic plateau in total surface coverage (curve 4) occurs when the instantaneous coverage of short chains reaches its maximum (curve 3). Furthermore, if one subtracts curve 3 from curve 4 to obtain the long chain coverage during coadsorption, curve 2 is recovered. This demonstrates that the rate of long chain coadsorption from the mixture is identical to its mass-transfer-limited noncompetitive adsorption rate.

From these observations, the following scenario becomes evident for the competitive coadsorption of the particular short–long chain combination of 33K and 120K: Initially, both short and long chains adsorb independently at their mass-transport-limited rates. This proceeds until the total mixed surface coverage reaches a level equal to the equilibrium coverage for the short chains alone. Beyond this time the long chains continue to adsorb at their mass-transport-limited rate, displacing the short chains on a mass-per-mass basis such that the total surface coverage remains constant during the exchange. Since the equilibrium coverage of the long chains exceeds that of the short chains, the final stage of coadsorption involves continued long chain adsorption, with increasing surface mass, until equilibrium coverage is attained.

Figure 3 also shows that the replacement of short chains by long ones takes place only after the surface appears saturated to the short chains. This means that there is no surface competition before this point and that the surface receives both species until it is saturated. This observation is qualitatively in accordance with the high affinity isotherms of both molecular weight samples,¹⁴ as predicted by the equilibrium theories⁴ for polymer chains with medium to high segmental adsorption energy.

For the particular combination of short and long chains presented thus far, the entire coadsorption process is transport-limited: In the early stages by the independent arrival of short and long chains to the interface, and in the late stages by the arrival of long chains to the interface. Therefore, the slopes of the rising and falling portions of curve 3 in Figure 3 represent the mass-transport-limited rates of the short

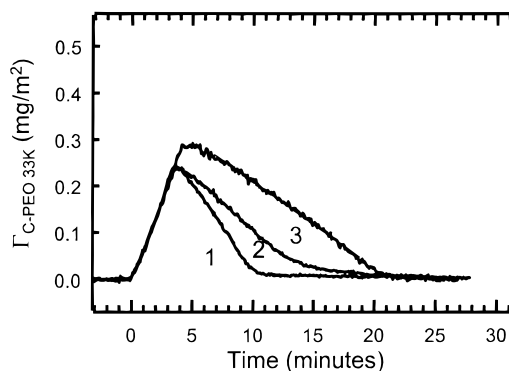


Figure 4. Coadsorption kinetics of the 33K C-PEO component of 50–50 wt % mixtures containing long chains of varied molecular weight: (curve 1) long chain molecular weight is 120K; (curve 2) long chains are 460K; (curve 3) long chains are 963K. Total bulk solution concentration is 5 ppm.

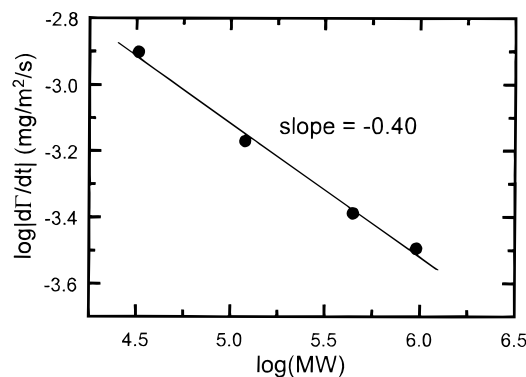


Figure 5. Rates of C-PEO adsorption/desorption during coadsorption. X-axis uses molecular weight of short chains for adsorption and molecular weights of long chains for desorption.

and long chains, as described by eq 1. In our experiments, the bulk solution mass concentrations are equal, which leads to

$$\frac{d\Gamma_i}{dt} \propto (D_i)^{2/3} \quad (2)$$

where i represents any adsorbing species.

Figure 4 shows the adsorption traces of 33K C-PEO during the coadsorption of binary mixtures (50–50 wt %) containing short 33K C-PEO chains and unlabeled long PEO chains whose molecular weights are varied: 120K, 448K, or 960K. From this we obtained the slopes $|d\Gamma/dt|$ (one rising, three falling) which should be proportional to the mass-transport-limited rates for the four molecular weights studied.

In Figure 5, the values of $|d\Gamma/dt|$ are plotted as a function of PEO molecular weight using a double-logarithm scale. A linear regression of the data yields the following relationship:

$$\frac{d\Gamma_i}{dt} \propto (MW)^{-0.4} \quad (3)$$

Combination of eqs 2 and 3 yields

$$D \propto (MW)^{-0.6} \quad (4)$$

The Stokes–Einstein equation provides a relationship between diffusivity and hydrodynamic radius, R_H :

$$D = \frac{kT}{6\mu R_H} \quad (5)$$

where k is the Boltzmann constant, T is the absolute temperature, and μ is the viscosity of water. Noting that $R_H \propto R_g^{21}$ where R_g is the radius of gyration of the polymer chain, a relationship is obtained between R_g and the molecular weight:

$$R_g \propto (\text{MW})^{0.6} \quad (6)$$

This result agrees well with the polymer solution theory for single polymer chains in a good solvent.

Our results, together with Dijt's findings¹¹ for adsorption from bimodal PEO mixtures containing 7K and 400K molecular weights, indicate that with pairs of short and long chains differing by at least a factor of 3 in length, and with short chains of 33K or less, the intrinsic short chain surface displacement step during the coadsorption was sufficiently rapid to yield bulk mass-transport control. Furthermore, the displacement of the temporally adsorbed short chains was virtually complete at long times (see Figure 4). These results also validate the prediction of the S-F equilibrium theory⁴ that long chains completely dominate the surface for this range of molecular weights and molecular weight differences.

(b) *Model of Competitive Polymer Adsorption.* The semiquantitative consistency of the competitive adsorption behavior seen thus far with transport-limited kinetics motivates a more quantitative treatment of competitive adsorption. Here we present a simple model for competitive adsorption, based on Langmuir equilibrium adsorption with a first-order surface rate, and diffusion of polymer chains from solution to the surface. Though this model contains no polymer physics, it captures the essential features of our observations and provides a benchmark for more complicated exchange processes more greatly influenced by interfacial relaxations.

One starts with a first-order adsorption process in which short or long chains can adsorb reversibly on surface sites:

$$\frac{dC_{\theta s}}{dt} = k_s C_s^* C_\theta - K_s C_{\theta s} \quad (7a)$$

$$\frac{dC_{\theta l}}{dt} = k_l C_l^* C_\theta - K_l' C_{\theta l} \quad (7b)$$

Here, C_θ , $C_{\theta s}$, and $C_{\theta l}$ are the concentrations of vacant surface sites, and those occupied by short and long chains, respectively. C_s^* and C_l^* are the concentrations of short and long chains in the fluid layer nearest the surface, while C_s and C_l without the asterisk designate the bulk solution polymer concentrations. Equations 7a and 7b include forward adsorption and reverse desorption reactions with forward rate constants k_s and k_l and reverse rate constants K_s and K_l' . While the distinct surface sites for short and long chains are physically ill-defined, the concept comes from the adsorption of smaller molecules. This simple treatment works adequately for polymer adsorption, since incorporation of polymer physics turns out not to be necessary, as will be shown. Clearly, large differences in the molecular weights of the adsorbing polymers will lead to distinct differences in the sizes of the footprints of adsorbed

chains of different lengths. It is, however, unnecessary to specify a difference in the sizes of the sites for short and long chains.

If each site represents some unit of the available surface area, then one can define T_l and T_s , the mass of polymer adsorbed per surface site, for long and short chains, respectively. Without incorporation of polymer physics to describe the relationship between fractional coverage and interfacial chain configuration, we treat T_l and T_s as constants based on the equilibrium coverage. The evolving surface mass can be calculated from the evolving surface site coverage according to

$$\frac{d\Gamma_s}{dt} = T_s \frac{dC_{\theta s}}{dt} \quad (8a)$$

$$\frac{d\Gamma_l}{dt} = T_l \frac{dC_{\theta l}}{dt} \quad (8b)$$

where Γ_l and Γ_s are the mass-based adsorbed amounts of long and short chains, respectively.

Equations 7a and 7b suggest the following equilibrium constants:

$$K_s = \frac{k_s}{K_s'} = \left(\frac{C_{\theta s}}{C_\theta C_s} \right)_{eq} \quad (9a)$$

$$K_l = \frac{k_l}{K_l'} = \left(\frac{C_{\theta l}}{C_\theta C_l} \right)_{eq} \quad (9b)$$

Also, the total number of surface sites is fixed, as governed by a surface site balance where $C_{\theta T}$ is the total concentration of surface sites.

$$C_{\theta T} = C_\theta + C_{\theta l} + C_{\theta s} \quad (10)$$

Before chains can adsorb to a surface, they must diffuse from the bulk solution to the interfacial region, a process described by mass transport coefficients M_s and M_l . These mass transport coefficients were measured experimentally for single species adsorption and found consistent with the solution to the Leveque equation (eq 1), for flow through a slit-shear cell.¹⁴

$$M_i = 0.538(\gamma D_i^2/L)^{1/3} \quad (11)$$

The flux of chains toward the surface must be consistent with their adsorption rate:

$$\frac{d\Gamma_s}{dt} = M_s(C_s - C_s^*) \quad (12a)$$

$$\frac{d\Gamma_l}{dt} = M_l(C_l - C_l^*) \quad (12b)$$

Combination of eqs 7–10 and 12 and restructuring into dimensionless form yield the rate equations for the evolving surface coverage by short and long chains.

$$\frac{d\theta_s}{d\tau} = \frac{F_s\theta - \theta_s/\alpha_s}{\beta_s + \theta} \quad (13a)$$

$$\frac{d\theta_l}{d\tau} = \frac{(M_l/M_s)(F_l\theta - \theta_l/\alpha_l)}{\beta_l + \theta} \quad (13b)$$

where θ_s , θ_l , and θ represent the fractional coverage of

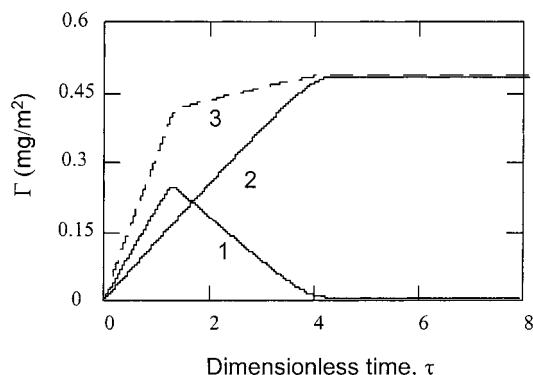


Figure 6. Predictions from eq 13 for the coadsorption experiment in Figure 3: a 50–50 wt % mixture of 33K and 120K PEO chains. Curves 1 and 2: surface mass traces of the short chain (33K) and long chain (120K), respectively. Curve 3: the total surface mass. The parameters chosen in the model are: $\alpha_1 = 6000$, $\alpha_s = 100$, $\beta_1 = \beta_s = 0$.

the surface by short chains, long chains, and the remaining fraction of the bare surface. F_s and F_l represent the fraction of short and long chains in the bulk solution.

In eqs 13a and 13b, the time has been made dimensionless according to

$$\tau = M_s C_T t / C_{\theta T} \quad (14)$$

with $C_T = C_s + C_l$, and the dimensionless equilibrium constants are

$$\alpha_s = K_s C_T \quad (15a)$$

$$\alpha_l = K_l C_T \quad (15b)$$

The β 's represent the relative rates of mass transport and surface kinetics:

$$\beta_s = M_s / (k_s C_{\theta T}) \quad (16a)$$

$$\beta_l = M_l / (k_l C_{\theta T}) \quad (16b)$$

Here, as β_1 and β_s approach zero, the process becomes transport limited. Variations in β allow quantification of deviation from transport-limited behavior in terms of the first-order rate constants k_s and k_l .

The parameters in eqs 13a and 13b were assigned values consistent with the adsorption experiment in Figure 3, and the equations were solved to provide perspective on coadsorption. First, the β -values were set to zero to yield transport-limited kinetics. Then the α -values were chosen to be large, corresponding to the high affinity adsorption of both PEO species.¹⁴ The α -value for the long chains was, however, chosen to be a factor of 30–60 greater than that for the short chains, such that the equilibrium would favor the long chains. Finally, the values of T_i were chosen to be 0.38 and 0.49 for short and long chains, respectively. These figures are based on the equilibrium coverages observed for noncompetitive adsorption of short and long chains: At conditions where the surface is nearly saturated, 0.38 and 0.49 mg/m² of short and long chains were observed.¹⁴

Figure 6 illustrates the results from these calculations, which are in quantitative agreement with the experimental data. Note that while there are many parameters that may appear to be adjustable in the

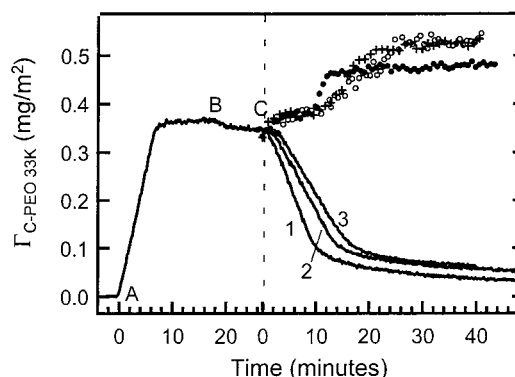


Figure 7. Sequential adsorption involving (A) preadsorption of 33K C-PEO at a bulk concentration of 2.5 ppm, (B) exposure of the layer to flowing buffer, and (C) exposure of the layer to 2.5 ppm unlabeled long chains. The total surface coverage during the long chain exposure is represented by symbols. The TIRF-measured displacement of short chains is represented by the numbered curves. Long chain molecular weights were (curve 1, ●) 120K, (curve 2, +) 460K, and (curve 3, ○) 963 K.

model, all of them must be chosen in accordance with the surface coverages for noncompetitive adsorption and the bulk solution diffusion coefficients that determine the individual mass transfer coefficients. Therefore, the agreement between theory and experiment emphasizes the simplicity of the physics of polymer coadsorption. The main difference between the simple theory and the experiment lies in the evolution of the total surface coverage during the displacement of the short chains by the longer ones. Experimentally, this is observed to occur at constant surface mass, while the Langmuir model predicts a linear increase in surface coverage at this stage of the process. Because the β -parameters have been set to zero in the calculation, the predicted evolution of the total surface mass reflects the shape of the mixed isotherm. S–F theory has shown constant total surface coverage in the mixed surface region of the binary isotherm. Indeed, the experimentally observed intermediate kinetic plateau in total surface coverage confirms the predictions of the S–F equilibrium theory and upholds Dijt's previous conclusions for local equilibrium during coadsorption with short chains of low molecular weight.¹¹

(c) Sequential Adsorption. Figure 7 shows the sequential adsorption experiments analogous to the coadsorption experiments in Figures 3 and 4. In Figure 7, short 33K C-PEO chains are preadsorbed from a bulk solution of 2.5 ppm and allowed to age briefly for a total contact time of 15 min with the polymer solution. Buffer is then passed through the flow cell at the same wall shear rate (7 s^{-1}) for 10 min, during which time no desorption occurs. The clock starts with the subsequent injection of unlabeled long chains. Figure 7 summarizes the results of several experiments where the long-chain molecular weight was varied: 120K, 463K, and 963K. Both reflectivity data for the evolving total surface mass and TIRF data for the displacement of the short chains are shown.

When long chains challenge a preadsorbed layer of shorter chains, the short chains are quickly displaced and initially exhibit a constant displacement rate roughly proportional to the molecular weight of the long chains to the 0.4 power, similar to the result in Figure 5. This observation suggests a transport-limited exchange during the linear decrease. In contrast to the coadsorption runs in Figures 3 and 4, the constant

displacement rate for the short chains gave way to a more gradual exchange process after about 80% of the short chains has been removed. Therefore, a significant population of the short chains resisted displacement in the sequential exchange experiment.

In Figure 7 the evolution of the total surface mass during the exchange was consistent with the displacement of the short chains and showed some similarities to the coadsorption kinetics in Figure 3. For each molecular weight of long chain considered, the transport-limited displacement of short chains proceeded at constant surface mass. The subsequent surface-controlled displacement of the more tightly bound short chains in the late stages of exchange coincided with an increase in the total surface coverage to a level more consistent with the equilibrium coverage of long chains. As the last 10–20% of the short chains were displaced, the total surface coverage increased very slightly.

Significant differences between the short chain history at the interface in coadsorption and sequential adsorption protocols may be responsible for the differences in the rate of short chain release (especially at long times) from the surface in these two types of experiments. In coadsorption experiments, the exchange process began with a relatively young (~ 4 min) mixed layer containing about 60–70 wt % short chains. In contrast, in the sequential runs, exchange began with a 25-min-old layer comprised entirely of short chains. Therefore, the average surface lifetime of short chains in the coadsorption experiment was significantly shorter than that in the sequential history. Also, the initially mixed layer in the coadsorption runs may be significant: If PEO chains possess sufficient lateral surface mobility, there may be continued competition between the short and long chains for strong and weak adsorption sites on the silica surface, which is surely heterogeneous. A second factor is that in the coadsorption experiment, the bulk solution always contained 2.5-ppm short chains such that short chains could self-exchange during the time they were displaced by long chains. This potential self-exchange of the short chains serves to further reduce the average surface lifetime of short chains at the interface in the coadsorption experiment.

2. Competitive Adsorption of 120K (Short) PEO and Longer Chains. The previous sections demonstrated that short chains of 33K molecular weight were overwhelmed by longer chains during competitive coadsorption and sequential adsorption. This section examines the dynamics of the competition between somewhat longer “short” chains (120K) and higher molecular weight long chains, still maintaining a factor of 3 or more difference between the short and long chain lengths.

(a) Coadsorption from Binary Mixtures. Figure 8 presents the coadsorption kinetics for 50–50 wt % mixtures containing 120K C-PEO chains and long unlabeled chains of 469K or 963K molecular weight. In addition to TIRF data for the short chain coverage, reflectivity data are presented for the evolving surface excess. As in previous experiments, the total bulk solution polymer concentration is 5 ppm, and the wall shear rate is 7 s^{-1} .

Figure 8 illustrates, for short chains of moderate molecular weight, initial coadsorption kinetics that follow independent bulk mass-transport control by the two components, similar to the results in Figure 3 with lower molecular weight short chains. After the initial

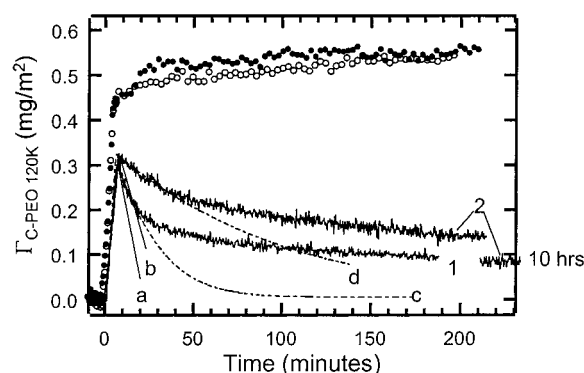


Figure 8. Competitive coadsorption kinetics for 50–50 wt % mixtures of 120K/460K (curve 1 and ●) and 120K/963K (curve 2 and ○) PEO pairs. The total concentration is 5 ppm. Curves 1 and 2 are the TIRF-measured kinetics of C-PEO 120K during the coadsorption. Symbol curves are the total surface mass measured by reflectivity. Lines a and b represent expectations for bulk-mass-transport-controlled displacement of short chains. Dashed lines c and d are the predictions from the model for (c) $\beta_1 = 0.02$, $\beta_s = 0.005$, and (d) $\beta_1 = 0.1$, $\beta_s = 0.005$.

mixed saturation of the surface in Figure 8, the subsequent replacement of short (120K) chains by longer ones is much slower than the transport-limited rate involving the arrival of long chains to the interface. (The solid straight lines in Figure 8 show the theoretical short chain replacement kinetics corresponding to bulk transport limitations.) Also shown are predictions for surface-limited processes that match both the adsorption kinetics and the initial displacement kinetics observed in the coadsorption experiments. The parameters giving the fit for the 120K/460K mixture were (curve c) $\alpha_1 = 3000$, $\alpha_s = 100$, $\beta_1 = 0.02$, and $\beta_s = 0.005$. Those corresponding to the 120K/963K mixture (curve d) were $\alpha_1 = 6000$, $\alpha_s = 100$, $\beta_1 = 0.1$, and $\beta_s = 0.005$. This range of β -values corresponds to a moderate influence of surface kinetics, still with some influence of bulk-transport-limited rate of chain arrival. Even so, the simple model agrees with experimental results only for the first 25% of the exchange process for the 120K/460K mixture and the first 10–15% of the exchange process of the 120K/963K mixture. The actual displacement rates for the short chains become continually slower, leaving significant amounts of short chains on the surface, even 3 h into the experiment. At 10 h of coadsorption, almost one-third of the originally adsorbed short chains remain for the 120K/963K mixture.

The reflectivity data in Figure 8 for the evolving total surface mass are distinctly different from the results in Figure 3. In Figure 8, an intermediate plateau occurs only briefly for the 120K/460K mixture, and not at all for 120K/963K mixture. As discussed by Dijt,¹¹ the intermediate kinetic plateau corresponds to the dilute region of the binary adsorption isotherm where both chain lengths coexist on the surface. As the surface composition changes (still maintaining local equilibrium), the total coverage does not. In the kinetic runs, the intermediate plateau therefore corresponds to portions of the process where local equilibrium is approached, perhaps for a few minutes in the early stages of the exchange process between 120K and 460K chains. The kinetic trapping of short chains on the surface corresponds to a slow increase in the total surface coverage, without an intermediate kinetic plateau, as seen at times longer than 15 min for both runs in Figure 8.

Table 1. Single Exponential Decay Time Constants of Short Chain Exchange

experiment	decay time constant (min)
coadsorption: from 50–50 wt % 120K/460K PEO mixture	393
coadsorption: from 50–50 wt % 120K/963K PEO mixture	418
sequential adsorption: preadsorbed 120K PEO layer challenged by 2.5 ppm 460K PEO solution	192
sequential adsorption: preadsorbed 120K PEO layer challenged by 2.5 ppm 963K PEO solution	197
sequential adsorption: preadsorbed 120K PEO layer challenged by 100 ppm 963K PEO solution	104

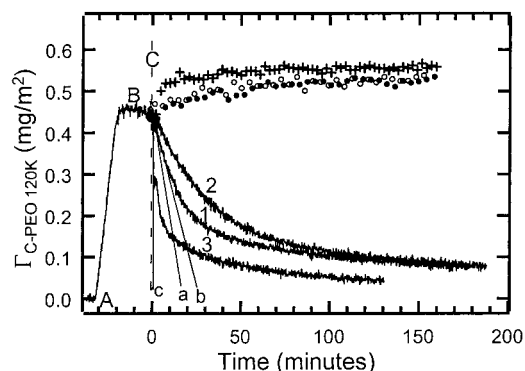


Figure 9. Sequential adsorption involving (A) preadsorption of 120K C-PEO at a bulk concentration of 2.5 ppm, (B) exposure of the layer to flowing buffer, and (C) exposure of the layer to unlabeled 460K long chains [(curve 1 & ○) 2.5 ppm bulk concentration] and 963 K long chains [(curve 2 & ●) 2.5 ppm bulk concentration, and (curve 3 & +) 100 bulk concentration]. The total surface coverage during the long chain exposure is represented by symbols. The TIRF-measured displacement of short chains is represented by the numbered curves. Lines a, b, and c represent expectations for bulk-mass-transport-controlled displacement of short chains (for the runs in curves 1, 2, and 3, respectively).

(b) *Sequential Adsorption.* The sequential adsorption experiments in Figure 9 follow a protocol similar to those in Figure 7: In Figure 9, 120K C-PEO chains are preadsorbed for 20 min. The layer is then contacted with flowing buffer for 10 min, during which time no desorption occurs. Next the preadsorbed 120K C-PEO chains are challenged with unlabeled solutions of long PEO chains, of 460K and 963K, with a bulk solution concentration of 2.5 ppm. To test the influence of the rate of long chain arrival (and the integrated short chains layer age) on the exchange rate, a more concentrated solution of 963K long chains is also used to challenge the preadsorbed layer.

The results in Figure 9 generally paralleled the trends in Figure 7 for lower molecular weight short chains; however, like Figure 8, Figure 9 shows the signature of significant deviations from local equilibrium. In Figures 3 and 7, for coadsorption and sequential competitive adsorption, the exchange of short and long chains occurred during periods of constant surface mass. In Figure 8, only one of the two curves shows a short period of exchange at constant surface mass. In Figure 9, the feature of constant surface mass has completely disappeared. In Figure 9, when preadsorbed 120K short chains are challenged by longer chains at a bulk solution concentration of 2.5 ppm, the short chain displacement is slow and corresponds to a slow increase in total surface mass that persists as long as short chains remain on the surface. In these runs, small amounts of preadsorbed short chains resist displacement for over 3 h.

In Figure 9, it is interesting to note that the short chain displacement rate is initially more rapid when the long chain arrival rate to the interface is raised by 2

orders of magnitude: Initially, the exchange of short chains and long chains occurs rapidly; however, the last 60% of the short chains still desorb at a rate that is surface-influenced. The more extensive rapid exchange of short and long chains in the initial stage of curve 3 may be a result of the overall shorter age of the preadsorbed layer. In sequential adsorption runs where the challenging species is relatively dilute in the bulk solution, its rate of arrival to the interface is slow and the preadsorbed layer continues to age while the exchange occurs. When the bulk solution concentration of the challenging chains is high, the exchange experiment is potentially shorter and the properties of the layer tend to evolve less during the exchange.

The surface-limited portions of the short chain displacement processes from Figures 8 and 9 were analyzed to determine if they followed single exponential or stretched exponential behavior. Such an analysis is meaningful only once the influence of transport on the overall kinetics is minimal, which occurs 10–15 min after the initiation of the decay. This analysis revealed, in all cases, decay behavior that was more nearly single exponential than stretched exponential. The time constants for these decays are tabulated in Table 1 and show a dependence on adsorption history (coadsorption vs sequential) and layer age (through the initial arrival rate of the long chains). The molecular weight of the long chains, for the studies conducted thus far, has minimal influence on the decay. The molecular weight of the short chains is surely important; however, the data for the lower molecular weight short chains in Figures 3 and 4 suggest an extremely fast surface time constant. The data in Figure 7 that show a strong surface influence represents only a small fraction of the layer, making quantitative analysis difficult. Notably, Granick observed single-exponential behavior for the self-exchange of polystyrene (with deuteriopolystyrene),²² while the stretched exponential kinetics were observed when weakly adsorbing chains were challenged with strongly adsorbed chains.^{7,23,24} Granick also found minimal influence of the molecular weight of the challenging chains in sequential adsorption studies.⁸ Our results are consistent with these observations, but warrant further investigation.

Stretched exponential behavior has been associated with nonequilibrium interfacial states^{23,24} and glassy relaxations,⁷ while single exponential decays are typically associated with behavior that maintains local equilibrium.⁸ Our results, which demonstrate a history dependence for the short chain displacement, argue that single exponential behavior can also be observed for cases dominated by metastable states. The situation in which a strongly adsorbing chain challenges more weakly adsorbing chains is different from the molecular-weight driven competition in this work, so different rate laws may be expected. Further, our results tend to suggest that the number of segment–surface contacts or entanglements among the interfacial chains is a critical piece of the puzzle. Our current understanding

of the situation leads us to focus more on the role of segment-surface contacts and their development with the age of the short chain layer, because the mixed surfaces generated by coadsorption have much more opportunity for overpinning of short chains by longer ones, or entanglements between short and long chains (e.g., in Figure 4), and yet transport-limited behavior can be observed to the point where all short chains are removed, if their time on the surface is sufficiently short.

Conclusions

The combination of TIRF and near-Brewster angle optical reflectivity has revealed the interfacial kinetics of individual PEO populations during competitive adsorption for mixtures containing different lengths of chains. A coadsorption history, in which both short and long chains occupied the surface at short times, was compared and contrasted with a sequential adsorption history, where a preadsorbed layer of short chains was later exposed to a solution of long chains. In both cases, when the short chains were on the order of 30K molecular weight, and their overall contact time with the surface was 5 min or less, their ultimate displacement by longer chains was fast (bulk-transport-limited) and nearly complete. For short chains of higher molecular weight, on the order of 120K, their displacement by even longer chains showed the influence of surface control: an energy barrier to remove the short chains from the surface. The displacement of these higher molecular weight short chains grew slower with time, compared with the predictions of a first-order Langmuir model, and obeyed kinetics that were single exponential. Further, the higher molecular weight short chains became more difficult to displace from the surface as their contact time at the interface was increased.

Acknowledgment. This work was sponsored by the National Science Foundation (CTS-929290 and CTS-9310932) and Whitaker Foundation grant to M. M. Santore.

References and Notes

- (1) Thies, C. *J. Phys. Chem.* **1996**, *70*, 3783.
- (2) Kolthoff, I. M.; Gutmacher, R. G. *J. Phys. Chem.* **1952**, *56*, 740.
- (3) Scheutjens, J. M. H. M.; Fleer, G. J. In *The Effects of Polymers on Dispersion Properties*; Tadros, Th. F.; Ed. Academic Press: London, 1981.
- (4) Fleer, G. J.; Cohen Stuart, M. A.; Scheutjens, J. M. H. M.; Cosgrove, T.; Vincent, B. *Polymers at Interfaces*; Chapman & Hall, 1993.
- (5) Pefferkorn, E.; Carroy, A.; Varoqui, R. *J. Polym. Sci. Part B* **1985**, *23*, 1997.
- (6) Pefferkorn, E.; Haouam, A.; Varoqui, R. *Macromolecules* **1989**, *22*, 2677.
- (7) Johnson, H. E.; Granick, S. *Science* **1992**, *255*, 966.
- (8) Frantz, P.; Granick, S. *Macromolecules* **1994**, *27*, 2553.
- (9) Schneider, H. M.; Granick, S. *Macromolecules* **1992**, *25*, 5054.
- (10) Enriquez, E. P.; Schneider, H. M.; Granick, S. *J. Polym. Sci. Part B* **1995**, *33*, 2429.
- (11) Dijt, J. C.; Cohen Stuart, M. A.; Fleer, G. J. *Macromolecules* **1994**, *27*, 3219.
- (12) Dijt, J. C.; Cohen Stuart, M. A.; Fleer, G. J. *Macromolecules* **1994**, *27*, 3229.
- (13) Dijt, J. C.; Cohen Stuart, M. A.; Hofman, J. E.; Fleer, G. J. *Colloids Surf.* **1990**, *51*, 141.
- (14) Fu, Z.; Santore, M. M. *Surf. Colloids A: Physicochem. Eng. Aspects* **1998**, *135*, 63.
- (15) Fu, Z.; Santore, M. M. *Macromolecules*, submitted.
- (16) Santore, M. M.; Fu, Z. *Macromolecules* **1997**, *30*, 8516.
- (17) Rebar, V. A.; Santore, M. M. *J. Colloid Interface Sci.* **1996**, *178*, 29.
- (18) Lide, D. R. Ed. *CRC Handbook of Chemistry and Physics*, 71st ed.; CRC Press: 1991; pp 8-34.
- (19) Santore, M. M.; Kelly, M. S.; Mubarekyan, E.; Rebar, V. A. In *Surfactant Adsorption and Surface Solubilization*; Sharma, R., Ed.; ACS Symposium Series 615; American Chemical Society: Washington, DC, 1995; Chapter 11.
- (20) Rebar, V. A.; Santore, M. M. *Macromolecules* **1996**, *29*, 6262.
- (21) Yamakawa H. *Modern Theory of Polymer Solutions*; Harper and Row: New York, 1971.
- (22) Frantz, P.; Granick, S. *Phys. Rev. Lett.* **1991**, *66*, 899.
- (23) Douglas, J. F.; Johnson, H. E.; Granick, S. *Science* **1993**, *262*, 2010.
- (24) Schneider, H. M.; Granick, S. *Macromolecules* **1994**, *27*, 4714.

MA980042W